The 2nd Spitzer Conference: Infrared Diagnostics of Galaxy Evolution
ASP Conference Series, Vol. 381, ©2008
Ranga-Ram Chary, Harry I. Teplitz, Kartik Sheth, eds.

Global Star Formation and Mid-Infrared Emission Features in Galaxies

Nanyao Lu and George Helou

Spitzer Science Center, MS 314-6, Caltech, Pasadena, CA 91125

Abstract. In view of the controversy as to whether the global aromatic features in emission (AFEs) can be used as a robust tracer of the current star formation in normal galaxies, we have constructed a simple two-temperature dust emission model consisting of a cold (diffuse) component of 20K and a warm component associated with star-forming regions. Based on a large sample of star-forming galaxies with available homogeneous *IRAS* infrared and *SCUBA* sub-mm fluxes, we show that both these dust components contribute to the global AFE emission. Only for very active star-forming galaxies (e.g., with *IRAS* $f_\nu(60\,\mu\mathrm{m})/f_\nu(100\,\mu\mathrm{m}) > 0.6$), does the star-forming component become dominant. We show that our model predictions are consistent with the *Spitzer* archival data in the case of the nearby galaxy NGC 6946.

1. Introduction

The mid-infrared aromatic features in emission (AFEs; also widely referred to as the PAH features) have recently been often used as a good tracer of the current star formation in galaxies, based mainly on their luminosity correlation with a known star-formation tracer such as Hα emission (e.g., Roussel et al. 2001; Wu et al. 2005). Nevertheless, it has been well known from *COBE* (e.g., Dwek et al. 1997), *ISO* (e.g., Lemke et al. 1998), *IRTS* (e.g., Chan et al. 2001) and *Spitzer* (e.g., Lu 2004) that AFEs arise plentifully in the general ISM and in Galactic sources devoid of a strong UV radiation field. Additional evidences for a significant diffuse AFE component include an apparent flux correlation of AFEs with the cold dust emission at 850 μm (Haas et al. 2002), *ISO* observations of normal galaxies (Lu et al. 2003; see their Fig. 9), and a morphological similarity in M33 between the diffuse AFEs and the dust emission at 160 μm (Rieke 2005, in this volume). In this article, we explore a simple two-component model for AFEs in galaxies and address the important question whether the global AFE emission is always dominated by the star-forming component in normal galaxies.

2. A Two-Component Model

From the *IRAS* survey we know that there are two characteristic dust temperatures in the ISM of normal galaxies. One is of T_w = 30-50 K associated with star-formation regions, and the other of $T_\mathrm{c} \approx 20$ K, typical of diffuse dust emission not directly associated with ionizing stars. In such a two-temperature picture, we can write

$$F_\mathrm{AFE} = a\,F_\mathrm{warm} + b\,F_\mathrm{cold}, \tag{1}$$

where F_AFE is the flux of AFEs, and F_warm (F_cold) is the integrated flux of the dust emission (not) associated with star formation. The coefficients a and

b depend on the spectral shape of the heating radiation field, the abundance ratio of the AFE carriers to large dust grains, and the intrinsic properties of the dust grains. For normal galaxies, it is not unreasonable to expect that the coefficient b varies only marginally from galaxy to galaxy (e.g., Helou, Ryter & Soifer 1991). On the other hand, the coefficient a for the warm component could vary significantly as the characteristics of the star-formation activity (the slope and upper-mass cutoff of IMF, age, etc.) could differ widely from galaxy to galaxy. Assuming an emissivity that scales as ν^2, we then have:

$$F_{\rm warm} = I_{\rm w} \int \nu^2 \, B(\nu, T_{\rm w}) \, d\nu, \quad \text{and} \tag{2}$$

$$F_{\rm cold} = I_{\rm c} \int \nu^2 \, B(\nu, T_{\rm c}) \, d\nu, \tag{3}$$

where $I_{\rm w}$ and $I_{\rm c}$ are proportional to the mass of their corresponding dust component, and $B(\nu, T)$ is the Planck function. Since the spectral shape of AFEs does not vary systematically for normal galaxies (e.g., Lu et al. 2003), we simply write $F_{\rm AFE} = \nu \, f_\nu$ at some frequency where AFEs are dominant. In this article, we use *IRAS* 12 μm flux density for its wide availability. (We will expand our analysis in a future study to using the more ideal IRAC 8 μm measurements from *Spitzer*.) To further simplify our model, we fix $T_{\rm c} = 20$ K. This leaves us with 3 free parameters: $I_{\rm w}$, $I_{\rm c}$, and $T_{\rm w}$, which we solve using the flux densities at 60 μm and 100 μm from *IRAS* and at 850 μm from *SCUBA* as these fluxes are the most uniformly available prior to *Spitzer*.

3. Model Results

We searched the literature for IRAS galaxies with available 850 μm fluxes. This generated 114 galaxies, with the 850 μm mostly from Dunne et al. (2000). We were able to obtain reasonable model solutions for all but 2 galaxies. The resulting $T_{\rm w}$ ranges from 30 to 50 K.

Fig. 1a is a plot of $F_{\rm AFE}/F_{\rm warm}$ *versus* $F_{\rm cold}/F_{\rm warm}$ for our sample galaxies. It appears reasonable to fit to the data points a linear correlation, for which the slope is the sample mean for the parameter b and the Y-axis intercept for a [see eq. (1)]. A least-squares fit gives $b = 0.29 \pm 0.03$ and $a = 0.13 \pm 0.02$. Subtracting the cold component, using the mean value of b above, from the total AFE flux we obtain Fig. 1b, a plot of the flux ratio of AFEs to the large grain emission for the warm component as a function of $T_{\rm w}$. Although there is a general trend here, the correlation is weak, suggesting that the intensity of the heating radiation field is probably not the primary driving force behind the scatter in Fig. 1b.

Fig. 2 plots the fractional AFE flux that is from the warm component as a function of *IRAS* 60 μm/100 μm flux density ratio. The statistical conclusion here is that, for many normal galaxies, the contribution from the cold component is significant. Only for very active star-forming galaxies (e.g., those with $f_\nu(60\,\mu{\rm m})/f_\nu(100\,\mu{\rm m}) > 0.6$), does the star-formation component become dominant. These claims remain valid even if we vary slightly the index of the power-law emissivity or $T_{\rm c}$ in our model.

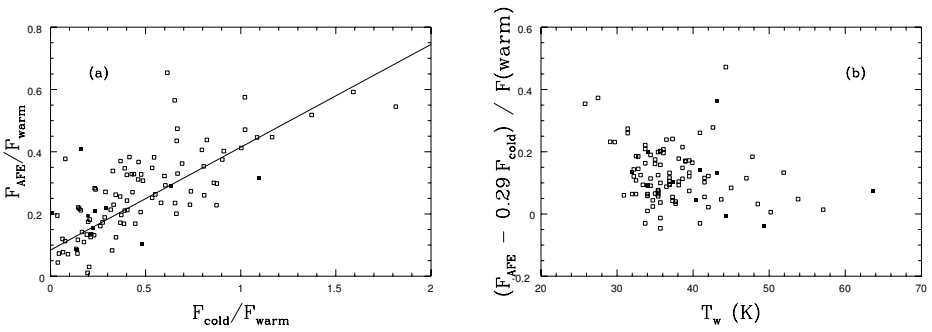

Figure 1. (a) $F_{\rm AFE}/F_{\rm warm}$ *vs.* $F_{\rm cold}/F_{\rm warm}$ for the *IRAS* sample galaxies. Solid squares are the sub-sample of 11 dwarf irregulars. The solid line is a least-squares fit to the whole sample. (b) $F_{\rm AFE}$ *vs.* $F_{\rm warm}$ as a function of the dust temperature for the warm component only. Symbols are the same as in (a).

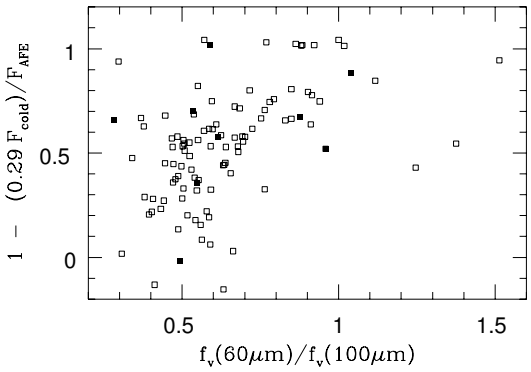

Figure 2. Percentage contribution to the AFEs from the warm dust component as a function of *IRAS* 60 μm/100 μm flux density ratio for our sample galaxies. Symbols are the same as in Fig. 1

4. Predictions for *Spitzer*

Our model predicts different ratios of $f_\nu(8\,\mu{\rm m})$ to a FIR flux density for the two dust components. Table 1 lists a few ratios relevant to *Spitzer* and *SCUBA* measurements. In reality, there is likely a continuous distribution of dust temperatures. But the ratios in Table 1 serve *roughly* as the limits between which the observed ratios should fall if our model is reasonably correct.

We compare Table 1 with *Spitzer* archive images of NGC 6946. In Fig. 3a the contours are for the surface brightness ratio of the (stellar photosphere-subtracted) IRAC 8 μm to MIPS 70 μm, overlaid on the MIPS 24 μm gray-scale image. There is a tendency for the red contours (ratios > 0.1) to lie between the 24 μm peaks. Fig. 3b is a plot of $I_\nu(8\,\mu{\rm m})/I_\nu(70\,\mu{\rm m})$ *vs.* log of $I_\nu(24\,\mu{\rm m})$ for a

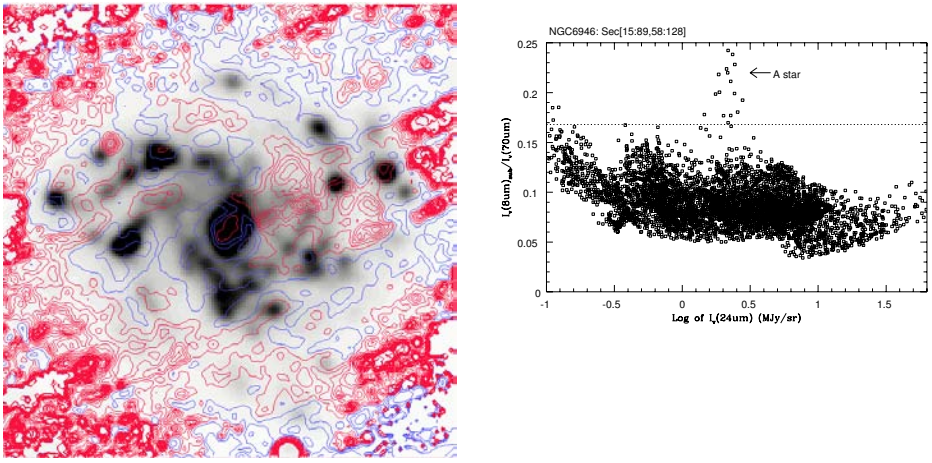

Figure 3. (a) (Left Panel) IRAC/MIPS pipeline data of the galaxy NGC 6946 from SINGS observations in *Spitzer* archive. $I_\nu(8\,\mu\mathrm{m})/I_\nu(70\,\mu\mathrm{m})$(contours) overlaid on the $24\,\mu$m gray image. The red and blue contours have ratios grater and less than 0.1, respectively. All the images have been smoothed to the same resolution. (b) (Right Panel) $I_\nu(8\,\mu\mathrm{m})/I_\nu(70\,\mu\mathrm{m})$ *vs.* log of $I_\nu(24\,\mu\mathrm{m})$ for the image pixels within a section of the galaxy disk left to the nucleus in (a). Some contamination from a foreground star is noted.

Table 1. Model Predictions

Component	$f_\nu(8\,\mu\mathrm{m})/f_\nu(70\,\mu\mathrm{m})$	$f_\nu(8\,\mu\mathrm{m})/f_\nu(160\,\mu\mathrm{m})$	$f_\nu(8\,\mu\mathrm{m})/f_\nu(850\,\mu\mathrm{m})$
Diffuse (20K)	0.17	0.032	2.0
SF (40K)	0.024	0.075	20
SF (50K)	0.033	0.17	58

section of the galaxy disk left to the nucleus in Fig. 3a, where the sky subtraction at $70\,\mu$m appears to be the most reliable. There is clearly a tendency for this ratio to rise as $I_\nu(24\,\mu\mathrm{m})$ decreases. Both this trend and the observed ratios agree well with our model predictions in Table 1.

References

Chan, K.-W., et al. 2001, ApJ, 546, 273.
Dunne, L, et al. 2000, MNRAS, 315,115.
Dwek, E., et al. 1997, ApJ, 475, 565.
Haas, M., Klaas, U., & Bianchi, S. 2002, A&A, 385, L23.
Helou, G., Ryter, C., & Soifer, B. T. 1991, ApJ, 376, 505.
Lemke, D., et al. 1998, A&A, 331, 742.
Lu, N. 2004, ApJS, 154, 286.
Lu, N., et al. 2003, ApJ, 588, 199.
Rieke, G. H. 2005, at *Extreme Starbursts: Near and Far; Lijiang, China, Nov 14-21.*
Roussel, H., Sauvage, M., Vigroux, L., & Bosma, A. 2001, A&A, 372, 427.
Wu, H., et al. 2005, ApJ, 632, L79.